THE ASTRONOMICAL JOURNAL, 119:681–687, 2000 February
© 2000. The American Astronomical Society. All rights reserved. Printed in U.S.A.

SUPERNOVA REMNANTS IN THE FOSSIL STARBURST IN M82[1]

RICHARD DE GRIJS, ROBERT W. O'CONNELL, GEORGE D. BECKER, AND ROGER A. CHEVALIER
Department of Astronomy, University of Virginia, P.O. Box 3818, Charlottesville, VA 22903-0818; grijs@virginia.edu, rwo@virginia.edu, gdb7s@virginia.edu, rac5x@virginia.edu

AND

JOHN S. GALLAGHER III
Department of Astronomy, University of Wisconsin, 475 North Charter Street, Madison, WI 53706; jsg@astro.wisc.edu
Received 1999 October 4; accepted 1999 October 27

ABSTRACT

We report the discovery of 10 compact Hα-bright sources in the poststarburst region northeast of the center of M82, called M82 B. These objects have Hα luminosities and sizes consistent with Type II supernova remnants (SNRs). They fall on the same Hα surface brightness–diameter relation (Σ-D) defined by SNRs in other nearby star-forming galaxies, with the M82 candidates lying preferentially at the small-diameter end. These are the first candidates for optically visible SNRs in M82 outside the heavily obscured central starburst within about 250 pc from the galactic center. If these sources are SNRs, they set an upper limit to the end of the starburst in region B2, about 500 pc from the galaxy's core, of about 50 Myr. Region B1, about 1000 pc from the core, lacks good SNR candidates and is evidently somewhat older. This suggests that star formation in the galaxy has propagated inward toward the present-day intense starburst core.

Key words: galaxies: evolution — galaxies: individual (M82) — galaxies: photometry — galaxies: starburst — supernova remnants

1. THE FOSSIL STARBURST IN M82

M82 is the nearest and best-studied starburst galaxy (for reviews, see Telesco 1988; Rieke et al. 1993). The active starburst has continued for $\lesssim$20 Myr at a rate of about 10 $M_\odot$ yr^{-1}. Energy and gas ejection from supernovae, at a rate of about 0.1 supernova yr^{-1} (O'Connell & Mangano 1978, hereafter OM78; Rieke et al. 1980), drive an Hα-bright galactic wind along the minor axis of M82 (e.g., Lynds & Sandage 1963; McCarthy, Heckman, & van Breugel 1987; Shopbell & Bland-Hawthorn 1998). The active starburst is located in the center of the galaxy, and this region has consequently received intense observational scrutiny. All of the bright radio and infrared sources associated with the active starburst are confined within a radius of about 250 pc. Most of this volume is heavily obscured by dust at optical wavelengths, although visible structures labeled M82 A, C, E, and F in the nomenclature of OM78, O'Connell et al. (1995), and Gallagher & Smith (1999) probably represent lower extinction parts of the outer starburst. The optical energy distributions of regions A and C indicate the presence of massive ionizing stars with ages of about 5 Myr (OM78; Marcum & O'Connell 1996), in agreement with ages based on infrared photometry for the higher extinction region of the starburst core (e.g., Rieke et al. 1993; Satyapal et al. 1997).

However, ample evidence exists that this is not the only major starburst episode to have occurred in M82. The high surface-brightness region M82 B, lying 500–1000 pc northeast from the galactic center, has exactly the properties one would predict for a poststarburst region in which an older starburst occurred with an amplitude similar to that of the active burst. Region B has an A-type absorption-line spectrum dominated by strong Balmer lines and lacks significant emission lines. Spectral synthesis (OM78; Marcum & O'Connell 1996) implies a sharp main-sequence cutoff corresponding to an age of about 100–200 Myr. Gallagher & Smith (1999) recently obtained an age of about 60 Myr for the very luminous ($M_V \sim -16$) cluster F, located 440 pc southwest of the galaxy's center. This suggests that active star formation has been propagating through the disk of M82 during about the last 100 Myr.

The present-day starburst core of M82 is well known to contain a large population of compact supernova remnants (SNRs). These are obscured at optical wavelengths by large line-of-sight extinction by dust, but their structures and evolution have been studied at radio wavelengths (e.g., Kronberg, Biermann, & Schwab 1985; Huang et al. 1994; Muxlow et al. 1994; Allen & Kronberg 1998). Heretofore, no SNRs have been detected at visible wavelengths in M82. In this paper we report the discovery of 10 SNR candidates in the "fossil" starburst region M82 B, based on narrowband Hα observations obtained with the *Hubble Space Telescope* (*HST*), and compare their properties with those of known SNRs in other star-forming galaxies.

2. Hα OBSERVATIONS AND DATA ANALYSIS

To supplement an ongoing broadband imaging program on super–star clusters in M82 B with the *HST* Wide Field Planetary Camera 2 (WFPC2) and *HST* Near Infrared Camera and Multi-Object Spectrometer (NICMOS), we extracted from the *HST* archive Hα + continuum observations of the central regions of M82, taken through the F656N narrowband filter (1997 March 16, program GO 6826, and 1995 September 1995, program GO 5957). These consisted of pairs of 500 and 300 s exposures, respectively. We combined the exposures to eliminate cosmic rays by

[1] Based on observations with the NASA/ESA *Hubble Space Telescope*, obtained at the Space Telescope Science Institute, which is operated by the Association of Universities for Research in Astronomy (AURA), Inc., under NASA contract NAS 5-26555.

using the IRAF/STSDAS[2] tasks MKDARK and COSMICRAYS. From these, we used IDL[3] to create an Hα + continuum mosaic of the central regions of M82 and coregistered this with our own broadband *HST* WFPC2 images in *V* (F555W) and *I* (F814W). Details of the latter observations (GO 7446) are discussed in de Grijs, O'Connell, & Gallagher (2000).

Since we lacked a suitable narrowband continuum image near the bandpass of the F656N filter, we created a pseudocontinuum image from our coregistered (and essentially emission-line–free) *V*- and *I*-band WFPC2 images by linearly interpolating the continuum fluxes to the mean wavelength of the F656N filter. We subtracted the pseudocontinuum image thus constructed from the Hα + continuum image to obtain an image containing pure line emission (the passband of the F656N filter is sufficiently narrow not to require an [N II] correction).

Figure 1 shows the regions of interest here on a ground-based *B*-band image of M82. Regions A and C are parts of the starburst core and lie at the base of the minor-axis Hα plume, which is not visible in this continuum image (OM78). The peak of the 2.2 μm continuum emission from the starburst core, often called the IR nucleus, lies 2″ west of the center of M82 A (Dietz et al. 1986; O'Connell et al. 1995). Region B lies northeast of A and C, separated from them by the strong central dust lane in the galaxy. The box in the image shows the area of M82 B that was imaged with *HST* in continuum bands by de Grijs et al. (2000). Because there is a gradient of properties within region B, we have divided it into two subregions, B1 and B2. The boundary between regions B1 and B2 is R.A.(J2000) = $9^h56^m00^s$, with B1 lying to the east of this line.

We based our flux calibrations on the procedures for WFPC2 data recommended by Holtzman et al. (1995). To check the quality of the resulting calibration, we compared the total Hα fluxes from the bright regions A and C (OM78) in the WFPC2 images with those obtained with 5.″8 circular-aperture, ground-based spectrophotometry by OM78. Aperture photometry of our images revealed the ground-based Hα values to be about 20% brighter than in the nominal WFPC2 calibration. Considering the various uncertainties, especially aperture-centering errors and our use of an interpolated continuum for correction of the *HST* emission-line data, this is good agreement. We will adopt the ground-based zero point for the Hα fluxes discussed in the remainder of this paper.

In the subsequent analysis, we adopt a distance of 3.6 Mpc or a distance modulus of $m-M = 27.8$ mag for M82, based on the Cepheid distance for M81 obtained by Freedman et al. (1994).

3. Hα EMISSION FROM THE FOSSIL STARBURST REGION

The *HST* pure Hα images, as well as ground-based images (e.g., Lynds & Sandage 1963; McCarthy et al. 1987), show that there is relatively little line emission in the disk of

[2] The Image Reduction and Analysis Facility (IRAF) is distributed by the National Optical Astronomy Observatories, which is operated by the Association of Universities for Research in Astronomy, Inc., under cooperative agreement with the National Science Foundation. STSDAS is the Space Telescope Science Data Analysis System; its tasks are complementary to the existing IRAF tasks.

[3] The Interactive Data Language (IDL®) is a registered trademark of Research Systems, Inc.

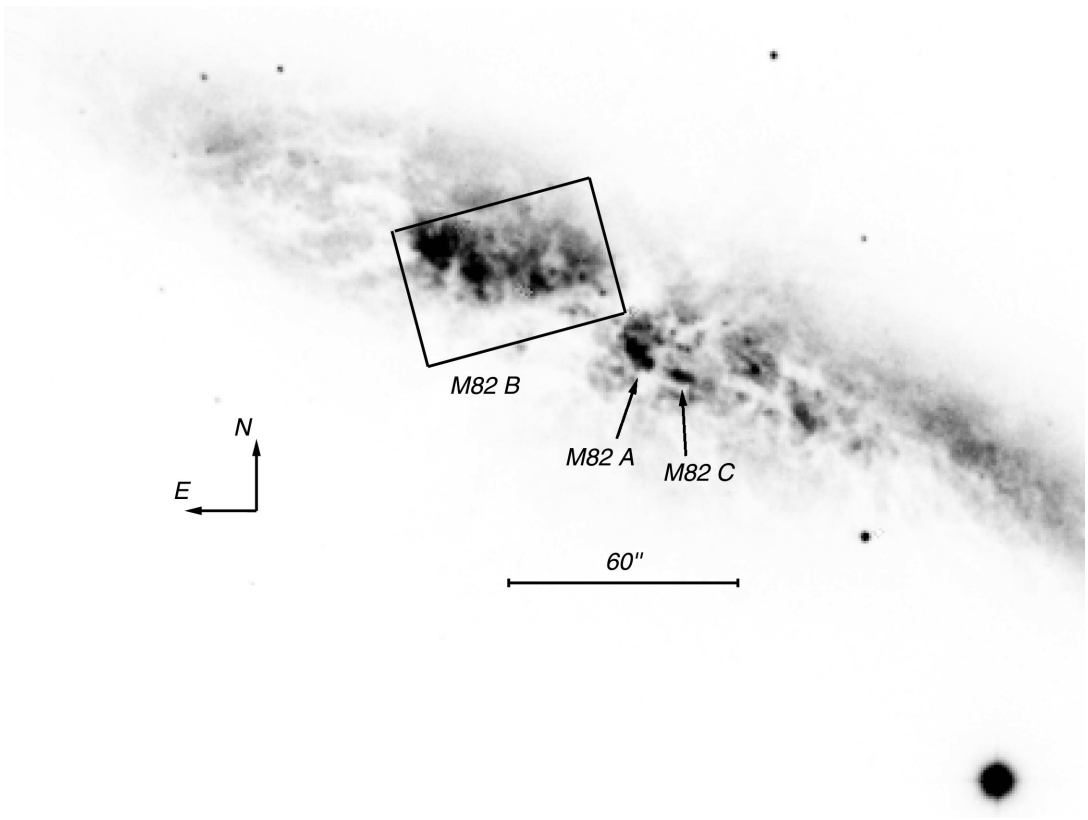


FIG. 1.—Palomar 5 m plate of M82 taken by Sandage in the *B* band (20 minutes, seeing $\lesssim 1''$), identifying the regions we discuss. North is at the top; 60″ corresponds to 1050 pc.

M82 at radii larger than 500 pc from the central starburst. The easily visible Hα is concentrated in the core starburst region and the bright minor-axis plume extending from it, perpendicular to the galaxy's disk.

Our continuum-subtracted pure Hα image of region B is shown in Figure 2*a*. There is diffuse Hα emission here, but at much lower levels than in regions A and C and in the bright plume. For a quantitative comparison, we integrated the Hα flux in our subtracted image over 20″ × 20″ apertures centered on regions A, B1, and B2. Total Hα luminosities were 2.6×10^{40}, 6.7×10^{38}, and 1.3×10^{39} ergs s^{-1}, respectively. The Hα surface brightness declines with distance from the galaxy's center.

Figure 2*b* shows the same field as Figure 2*a* in the continuum *I* band. A bright diffuse stellar background is present, and several dozen individual compact star clusters are visible. (The clusters are discussed further in de Grijs et al. 2000.) There is clearly not a one-to-one correspondence between the clusters and the bright emission-line regions. Many clusters have little or no Hα emission, and some Hα emission regions have inconspicuous continuum counterparts.

Figure 2*a* shows that region B1 has few compact Hα sources. However, B2, located closer to the active starburst core, is brighter in Hα, as a result of both compact sources and diffuse emission, although still at a surface brightness

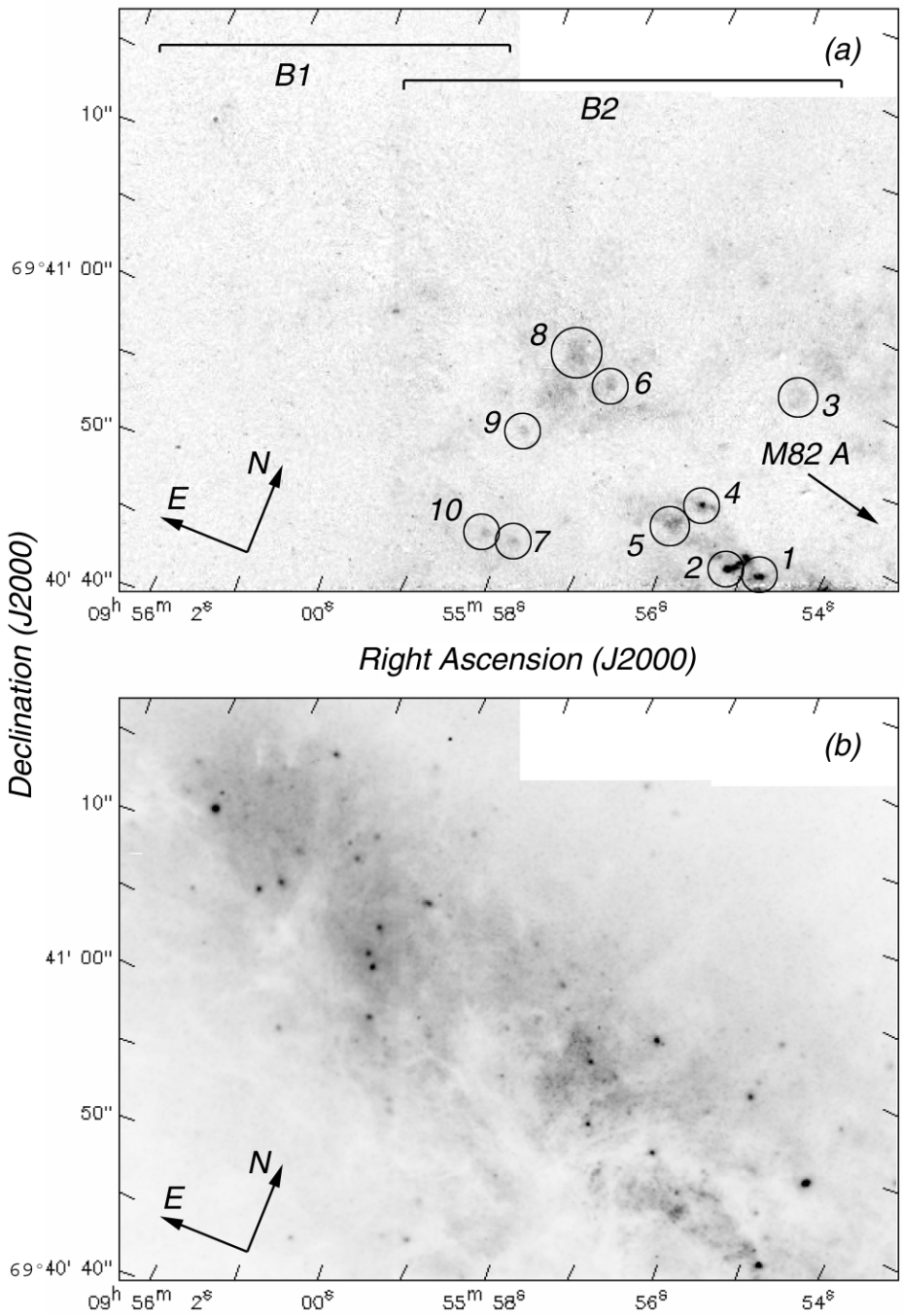


FIG. 2.—*HST* WFPC2 images of the M82 B region outlined in Fig. 1 (resolution 0.″1), but with a different orientation. The 5″ bar corresponds to 88 pc. (*a*) Continuum-subtracted Hα image. The SNR candidates discussed in this paper are circled. Numbers correspond to those in Table 1. (*b*) *I*-band image of same region as in (*a*), showing numerous compact star clusters, the bright diffuse background, and dust lanes.

20 times lower than that of the active starburst. We used the FIND routine in DAOPHOT (Stetson 1987) to identify compact sources on both the emission-line and continuum images. We measured net fluxes for these using circular apertures with radii in the range 3–7.5 pixels (0.″30–0.″75), adjusted depending on the structure and brightness of the local background. We obtained Hα fluxes and equivalent widths (EWs) for, respectively, 37 and 50 compact optical continuum sources in B1 and B2 (cf. de Grijs et al. 2000), of which only nine and 16, respectively, contain significant Hα emission. Positive Hα detections are listed in Table 1.

Most of the identified Hα sources in B2 have Hα brightnesses significantly above the norm for the exterior regions of the galaxy, especially considering the excess extinction in B2 (estimated to have $A_V \sim 1.1 \pm 0.3$ mag higher than B1; de Grijs et al. 2000). The brightest object in B2 resolves to a "string of pearls" of discrete sources and is conspicuously located adjacent to the strong central dust lane, which separates region B from the starburst core.

In addition to Hα associated with definite, compact continuum sources, we found 11 Hα compact sources in region B2 with only faint counterparts in the continuum passbands. We measured fluxes for these as above. Net continuum fluxes were positive, if small, in all cases, yielding equivalent widths of 50 Å or higher. These sources are listed in Table 1 with asterisks. The quoted errors for the EWs include the estimated statistical uncertainties in the continuum measures.

One expects to find two types of compact Hα sources in a galaxy like M82. H II regions will exist around young star clusters with ages $\lesssim 10$ Myr by virtue of the presence of ionizing O- or early B-type stars. Although very young H II regions can have substantial Hα EWs in the range 100–1000 Å (e.g., Bresolin & Kennicutt 1997), there should always be a significant continuum source associated with these, even if there is considerable extinction in the vicinity. Type II supernovae (SNe) can also produce compact Hα remnants. These will often be associated with their parent star clusters,

TABLE 1

COMPACT Hα SOURCES IN M82B

Source Number[a]	R.A. (J2000.0)	Decl. (J2000.0)	L(Hα) (10^{35} ergs s^{-1})	$\langle\Sigma_{H\alpha}\rangle \times 10^{-16}$ (ergs s^{-1} cm^{-2} arcsec^{-2})	EW (Å)	FWHM$_{H\alpha}$ (pc)
Supernova Remnant Candidates						
1	09 55 54.71	69 40 55.6	56.8 ± 3.5	86.7 ± 5.3	41.5 ± 2.6	5.3
2	09 55 55.17	69 40 55.3	91.0 ± 2.2	138.9 ± 3.4	354.1 ± 8.6	3.6
*3	09 55 55.17	69 41 06.5	35.6 ± 1.8	11.4 ± 0.6	50.1 ± 4.5	18.4
4	09 55 55.77	69 40 58.7	38.2 ± 2.6	58.3 ± 4.0	101.7 ± 6.8	6.4
5	09 55 55.98	69 40 57 0	32.5 ± 2.2	31.8 ± 2.2	26.8 ± 1.9	12.2
*6	09 55 57.48	69 41 03.1	23.8 ± 1.2	23.8 ± 1.2	60.8 ± 13.5	8.3
*7	09 55 58.03	69 40 51.1	14.3 ± 0.8	18.2 ± 1.0	108.9 ± 23.8	7.1
*8	09 55 58.03	69 41 04.5	19.0 ± 1.7	15.3 ± 1.4	51.6 ± 15.1	13.7
*9	09 55 58.36	69 40 58.4	16.0 ± 0.8	20.4 ± 1.0	570.1 ± 444.5	7.7
*10	09 55 58.42	69 40 51 2	14.2 ± 0.7	18.1 ± 0.9	214.8 ± 65.0	7.9
Other Hα Sources						
11	09 55 53.95	69 41 11.1	4.2 ± 1.7	2.8 ± 1.1	7.4 ± 2.9	...
12	09 55 54.33	69 41 06 1	1.8 ± 1.0	2.7 ± 1.5	6.6 ± 3.6	2.5
13	09 55 54.46	69 40 56.9	7.5 ± 0.8	15.0 ± 1.6	54.1 ± 5.6	5.6
*14	09 55 54.74	69 40 12 5	2.2 ± 1.0	3.7 ± 1.7	114.6 ± 75.2	7.2
15	09 55 54.77	69 40 57 6	1.2 ± 1.1	1.2 ± 1.1	2.6 ± 2.5	...
16	09 55 55.14	69 41 09.8	1.6 ± 1.0	2.4 ± 1.5	6.6 ± 4.1	2.0
*17	09 55 55.85	69 41 01 7	7.9 ± 0.5	17.6 ± 1.1	135.0 ± 40.5	...
*18	09 55 56.07	69 41 13.3	8.9 ± 0.8	11.4 ± 1.0	307.1 ± 126.9	7.4
19	09 55 56.48	69 40 57.2	0.9 ± 0.7	2.4 ± 1.9	13.6 ± 9.9	6.4
*20	09 55 56.82	69 40 14 0	5.7 ± 0.6	7.3 ± 0.8	126.5 ± 45.0	6.9
21	09 55 57.15	69 40 57 6	5.2 ± 1.2	5.1 ± 1.2	9.7 ± 2.2	2.8
*22	09 55 57.45	69 40 53.7	5.2 ± 0.5	11.6 ± 1.1	292.2 ± 167.4	6.5
23	09 55 57.46	69 41 00.3	5.3 ± 1.8	5.2 ± 1.8	7.5 ± 2.5	6.0
24	09 55 57.60	69 40 59.7	1.8 ± 0.6	4.9 ± 1.6	38.3 ± 13.6	2.7
25	09 55 58.01	69 41 12.6	1.4 ± 0.6	2.8 ± 1.2	8.0 ± 3.5	4.0
26	09 55 58.71	69 40 58.4	2.3 ± 0.7	4.6 ± 1.4	13.5 ± 4.2	3.6
27	09 55 59.07	69 41 07.1	1.6 ± 0.6	4.3 ± 1.6	19.5 ± 7.1	1.7
28	09 56 00.02	69 41 01.6	4.6 ± 0.9	7.0 ± 1.4	22.2 ± 4.2	1.9
29	09 56 00.84	69 41 08 4	1.9 ± 0.9	2.9 ± 1.4	2.0 ± 0.9	2.6
30	09 56 00.84	69 41 19 8	1.1 ± 0.6	1.6 ± 0.9	94.6 ± 52.5	2.8
31	09 56 01.25	69 41 14 1	4.3 ± 1.0	6.6 ± 1.5	8.6 ± 2.1	2.7
32	09 56 01.67	69 41 07 3	1.8 ± 0.6	2.8 ± 0.9	9.3 ± 3.1	3.3
33	09 56 03.28	69 41 06 7	4.6 ± 1.0	7.0 ± 1.5	18.4 ± 3.8	3.8
34	09 56 03.33	69 41 13 4	2.0 ± 1.0	5.5 ± 2.8	5.3 ± 2.5	4.8
35	09 56 03.34	69 41 12 2	8.8 ± 1.4	8.6 ± 1.4	3.4 ± 0.6	2.9
36	09 56 03.75	69 41 12 8	1.4 ± 0.7	2.9 ± 1.5	7.9 ± 3.9	3.2

NOTE.—Units of right ascension are hours, minutes, and seconds, and units of declination are degrees, arcminutes, and arcseconds.

[a] An asterisk indicates a source with only a faint optical continuum counterpart.

but in many cases there may be no well-defined compact continuum source. Since Type II SNe can occur up to 50 Myr after a star formation event, the associated cluster may have faded or dynamically expanded enough to be inconspicuous against the bright background of the galaxy. Alternatively, the parent star of the SNR could have been ejected from the cluster or could have formed initially in the lower density field. In fact, earlier studies of resolved starbursts suggest that 80%–90% of the bright stellar population resides in a diffuse component outside of compact clusters (e.g., Meurer et al. 1995; O'Connell et al. 1995).

The identified M82 B Hα sources fall into two wide luminosity ranges: those with $L(\mathrm{H}\alpha) < 9 \times 10^{35}$ ergs s^{-1} and those with $L(\mathrm{H}\alpha) > 14 \times 10^{35}$ ergs s^{-1}. Neither group has the properties expected for normal H II regions in the disk of a late-type galaxy. Recent samples of normal H II regions in spiral and irregular galaxies have been compiled by Kennicutt, Edgar, & Hodge (1989), Bresolin & Kennicutt (1997), and Youngblood & Hunter (1999), among others. The brightest Hα source in M82 B has $L(H\alpha) < 10^{37}$ ergs s^{-1}. Although normal galaxies contain many H II regions with luminosities in this range, they also invariably have much brighter sources, with luminosities up to 10^{38} or 10^{39}ergs s^{-1}. The largest M82 B source is smaller than 20 pc in diameter, whereas typical diameters for normal disk H II regions are 30–100 pc.

Instead, we believe that the 10 sources in the more luminous group are good candidates for SNRs. These are listed in the upper part of Table 1. Six of these have only faint counterparts in the continuum passbands. Some of the sources (e.g., source 3 in Fig. 2*a*) show evidence of limb brightening, as might be expected for older supernova remnants.

4. SNR CANDIDATES IN M82 B

Hα observations of large numbers of SNRs have recently become available for a number of nearby galaxies. In this section, we compare the properties of our M82 candidate SNRs with those of this larger sample. We consider Hα luminosities, sizes, and surface brightnesses.

Figure 3 shows that the Hα luminosities of the SNR candidates in M82 B (uncorrected for either foreground or internal extinction) are consistent with those of the main populations of SNRs in similar galaxies. In this figure, we have collected the Hα luminosities of SNRs in three late-type galaxies (Blair & Long 1997; Matonick, Fesen, Blair, & Long 1997), as well as for M81, the luminous Sb-type neighbor of M82. The M82 values fall at the low end of the plotted range, overlapping the SNRs in NGC 300 and M81. However, a correction for the obvious, if not well-determined, internal extinction in region B (probably a factor of about 1.5–2.0 at 6500 Å) would produce better agreement with the mean of the distribution. Although we have chosen these four comparison systems as most relevant to possible SNRs in M82, the luminosities plotted are typical of the complete sample of SNRs known in nearby galaxies, including M31, M33, M101, and the Large Magellanic Cloud (Long et al. 1990; Braun & Walterbos 1993; Yang, Skillman, & Sramek 1994; Matonick & Fesen 1997; Gordon et al. 1998).

A comparison of the physical FWHMs of our SNR candidates (see Table 1) with those of the Hα emission in the comparison samples reveals that the M82 sources are relatively small, with sizes averaging 10 pc compared with

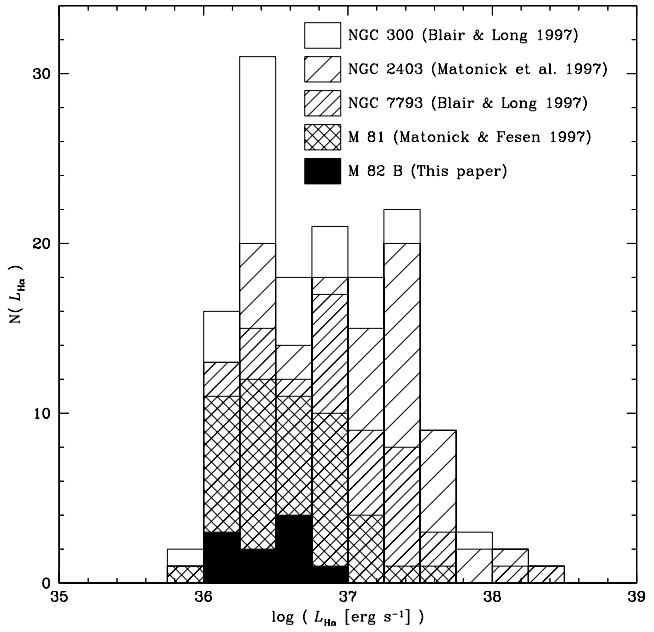


FIG. 3.—Histogram of Hα luminosities for SNRs in a sample of normal nearby disk galaxies compared with those for our M82 SNR candidates. No extinction corrections have been applied to the M82 values.

values of over 50 pc in typical spiral galaxies (see Fig. 4). The M82 B candidates are, however, larger than the bona fide SNR sources in the central starburst of M82, which have radio continuum diameters in the range 1–5 pc. We return to the question of the sizes of our candidates in § 5.

Surface brightness–diameter relations (Σ-*D* relations) in the radio continuum have formed the basis of many SNR studies; they were first discussed for Galactic radio SNRs by Woltjer (1972) and Clark & Caswell (1976). At radio wavelengths, the Σ-*D* relations for the Galaxy, the LMC, and other galaxies, including M82 (Berkhuijsen 1986; Huang et al. 1994; Muxlow et al. 1994), superpose suffi-

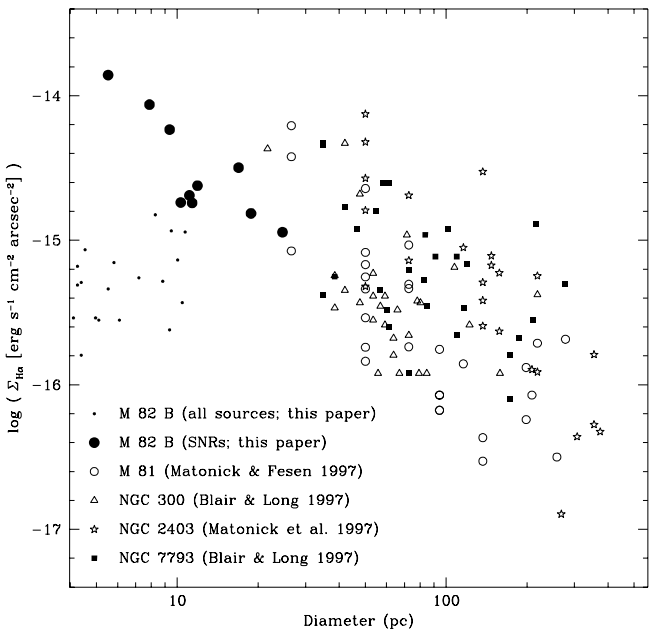


FIG. 4.—Composite Hα surface brightness–diameter relation for the SNR candidates in M82 B and for the normal SNR sample in Fig. 3.

ciently well to construct a composite Σ-D relation with relatively small scatter for all known shell radio SNRs (e.g., Milne, Caswell, & Haynes 1980; Berkhuijsen 1983, 1986; Green 1984; Case & Bhattacharya 1998).

Σ-D relations in Hα have been discussed before only in the context of the young SNRs in M33 (Long et al. 1990; Gordon et al. 1998). In Figure 4, we plot the Hα surface brightnesses and diameters for the candidate SNRs in M82 and for a composite comparison sample. Surface brightnesses (Σ) are computed in units of ergs s^{-1} cm^{-2} arcsec^{-2} and are tabulated for our candidates in Table 1. The comparison sample includes the same systems shown in Figure 3. Figure 4 shows that a broad Hα Σ-D relation exists for SNRs in normal late-type galaxies. Although the Hα surface brightnesses of the M82 candidates are generally high and the diameters small, they fall on the same (Σ-D) relation as do the normal SNR samples. This is additional evidence supporting the interpretation of the M82 candidates as SNRs.

High-resolution Very Large Array (VLA) observations at 8.4 GHz of the M82 central regions were obtained by Huang et al. (1994), with a total integration time of 20 minutes, of which the appropriate section covering M82 B was kindly made available to us by J. Condon. None of the Hα-bright SNR candidates, with the possible exception of source 2 (cf. Fig. 2*a*), appear to show 8.4 GHz radio emission brighter than about 300 μJy associated with them. However, the string of pearls of bright, discrete Hα sources in the southwestern corner of our field seems to be an extension of a similar string of bright 8.4 GHz sources lying behind the strong dust lane just outside our Hα field of view that crosses the galaxy near this position (see Fig. 1). Likewise, most of the bright 8.4 GHz sources in region B2 are located in areas with higher than average extinction, where detection of optical or Hα counterparts would be difficult. Deeper imaging at radio wavelengths may result in positive detections at lower radio continuum flux limits; because of the steep spectral index of SNRs, imaging at lower frequencies would be preferable.

It is not unusual for SNRs to be Hα bright while lacking significant emission at radio wavelengths. From a theoretical point of view, radio and Hα emission are due to different physical processes and are prominent at different evolutionary stages of the SNR. Radio emission arises earlier in SNR evolution than does Hα emission.

M31 (Braun & Walterbos 1993) and M33 (Gordon et al. 1998) are the only galaxies in which optically selected SNRs have been studied in detail at radio wavelengths. Of the approximately 150 optically selected SNRs and SNR candidates in M31 and M33, about 40% are not detected above about 200 μJy. Fluxes from similar SNRs in M82 would be expected to be about 10 times fainter than those in M31 and M33, so the absence of such radio emission from the M82 B candidates does not appear to be unusual. By contrast, the brightness of the SNRs in the M82 starburst core (cf. Huang et al. 1994) may be a product of an abnormally dense interstellar medium.

5. EVOLUTIONARY STATE OF THE M82 B SUPERNOVA REMNANTS

Strong Hα emission from an SNR ordinarily implies that it is in a radiative evolutionary state. Hα is observed from nonradiative remnants, such as Tycho's remnant, but the emission is weak. Assuming evolution in a constant-density interstellar medium, the radiative state at a particular radius implies a lower limit for the ambient density. Cioffi, McKee, & Bertschinger (1988) give expressions for the radius and velocity at which the radiative PDS (pressure-driven snowplow) phase begins: $R_{\rm PDS} = 5.2\ E_{51}^{2/7} n_1^{-3/7}$ pc and $v_{\rm PDS} = 574\ E_{51}^{1/14} n_1^{1/7}$ km s^{-1}, where E_{51} is the supernova energy in units of 10^{51} ergs and n_1 is the hydrogen density in units of 10 cm^{-3}. These expressions assume solar metallicity, which is appropriate for M82 (OM78). By using the smallest diameter, 5.5 pc, and taking a standard SN energy, $E_{51} = 1$, the minimum density is 44 cm^{-3}. The shock velocity in such a remnant is 710 km s^{-1} at the time of shell formation. The required density is not unusual for a dense cloud, especially in an active star formation region.

An alternative to interstellar interaction is interaction with presupernova mass loss. The expectation for the SNRs in M82 B is that their progenitors are at the low-mass end of Type II SN progenitors and thus are approximately B1–B3 stars when on the main sequence. These stars are too cool to have strong winds. They may have slow, dense winds as red supergiant stars, but at the radii of interest here the density is not expected to be sufficiently high to sustain a radiative shock front. Interstellar interaction is the more likely situation.

Models of radiative shock waves show that the Hα intensity is $\propto n_o v_{\rm sh}^2$, where n_o is the ambient density and $v_{\rm sh}$ is the shock velocity, if $v_{\rm sh}$ is in the approximate range 100–200 km s^{-1} and the shocked gas is preionized (Raymond 1979). The dependence on $v_{\rm sh}$ is probably weaker at higher shock velocities and may tend to $\propto n_o v_{\rm sh}$. The expansion of a radiative remnant can be approximated by $v_{\rm sh} \propto n_o^{-0.8} R^{-2.2}$ for a fixed explosion energy (Chevalier 1974; Cioffi et al. 1988), where R is the radius of the SNR. The implied Σ-D relation for Hα is then $\Sigma \propto n_o^{-0.6} D^{-4.4}$, perhaps tending to $\Sigma \propto n_o^{0.2} D^{-2.2}$ at high shock velocities. For a fixed density, this relation is considerably steeper than the observed relation shown in Figure 4. One reason for this may be observational selection: the observed sample may consist of SNRs for a range of ambient density that have just become radiative and are therefore brightest. They subsequently fade from view and fall below the detection threshold. Another reason may be that the expansion takes place in an inhomogeneous medium and only a small part of the shell has become radiative for the apparently small remnants.

The relation of these possible SNRs to the smaller, nonthermal radio-emitting remnants in the center of M82 is unclear. The central remnants are not observed in optical-line emission, so it is unknown whether they are in a radiative phase of evolution. These remnants probably have more massive stars as progenitors and so could have a complex mass-loss environment. Finally, the higher interstellar pressure in the center of M82 could lead to different evolutionary properties.

6. INFERRED AGE OF THE POSTSTARBURST REGIONS

The presence of SNRs in the poststarburst region of M82 can help to set limits on its star formation history. The last SNe in a quenched starburst region would occur at a time comparable with the longest lifetime of an SN progenitor after the end of the starburst activity. Following Iben & Laughlin (1989) and Hansen & Kawaler (1994), the time t spent between the zero-age main-sequence and planetary nebula phase by an 8 $M_\odot$ progenitor star, which is generally adopted as a lower limit for Type II SNe (e.g., Kennicutt

1984), corresponds to $t \sim 35$–55 Myr. Type Ia SNe, which involve lower mass stars in binary systems, can occur much later, but one expects these to be more uniformly distributed over the galaxy's surface, not concentrated near regions of recent star formation.

The radiative lifetimes of the shell SNRs in their later phases are short in this context. They are limited by the expansion velocities of their shells. Older SNRs will be physically large and have low surface brightnesses. Radio observations of well-studied Galactic SNRs indicate relatively rapid luminosity declines, causing the observable radiative SNR lifetimes to be about 10^4–10^6 yr (e.g., Braun, Goss, & Lyne 1989; Shull, Fesen, & Saken 1989; Matthews, Wallace, & Taylor 1998), at which time they will have attained diameters of order 50–100 pc.

Therefore, if our candidates are indeed SNRs, they suggest an upper limit to the end of the starburst event in region B2 of about 50 Myr. The absence of SNR candidates in B1 indicates it is older. The spectral synthesis dating of region B1 is consistent with this ($\sim$100–200 Myr; Marcum & O'Connell 1996), as are the colors of the *HST*-detected star clusters (de Grijs et al. 2000). There is then the following progression of ages with distance from the center of the current starburst: B1 ($\gtrsim$100 Myr, $r \sim 1000$ pc), B2 ($\lesssim$50 Myr, $r \sim 500$ pc), and the present core (active for $\lesssim$20 Myr, $r < 250$ pc).

7. SUMMARY AND CONCLUSION

We have studied the Hα emission from the poststarburst region 500–1000 pc northeast of the center of M82 by using *HST* WFPC2 images. Hα emission in this region in general is far below levels associated with the current starburst core within about 250 pc from the galactic center. Region B1 has little diffuse emission and few compact sources. Region B2, located closer to the core, has more of both. We find that the compact sources divide by Hα luminosity into two groups. The objects in the brighter group are good candidates for Type II supernova remnants. Their Hα luminosities, surface brightnesses, and sizes are consistent with those of SNRs in other star-forming galaxies. We attribute their smaller sizes and higher surface brightnesses to a relatively higher local interstellar gas density (~ 50 cm^{-3}) than prevails in normal spiral disks.

If these candidates are indeed SNRs, they indicate an upper limit to the end of the starburst event in region B2 of about 50 Myr and suggest that intense star-forming activity in M82 has propagated inward toward the present starburst core during the past 100–200 Myr.

The evidence that our candidates are actually SNRs is only circumstantial. Although their properties seem to compare better with SNR samples in other galaxies than to those of H II regions, they could be H II regions that have been affected by the unusual physical circumstances in the disk of M82. A straightforward test would be to obtain [S II]/Hα emission-line ratios for the candidates, since these are sensitive to the presence of strong shock waves.

This work is based on the undergraduate senior thesis of G. Becker at the University of Virginia. We are grateful to A. Sandage for the loan of the plate reproduced in Figure 1 and to J. Condon for a radio map of M82 B. We also acknowledge insightful discussions with Z.-Y. Li. This research was supported by NASA grants NAG 5-3428, NAG 5-6403, and NAG 5-8232.

REFERENCES

Allen, M. L., & Kronberg, P. P. 1998, ApJ, 502, 218
Berkhuijsen, E. M. 1983, A&A, 120, 147
———. 1986, A&A, 166, 257
Blair, W. P., & Long, K. S. 1997, ApJS, 108, 261
Braun, R., Goss, W. M., & Lyne, A. G. 1989, ApJ, 340, 555
Braun, R., & Walterbos, R. A. M. 1993, A&AS, 98, 327
Bresolin, F., & Kennicutt, R. C. 1997, AJ, 113, 975
Case, G., & Bhattacharya, D. 1998, ApJ, 504, 761
Chevalier, R. A. 1974, ApJ, 188, 501
Cioffi, D. F., McKee, C. F., & Bertschinger, E. 1988, ApJ, 334, 252
Clark, D. J., & Caswell, J. L. 1976, MNRAS, 174, 267
de Grijs, R., O'Connell, R. W., & Gallagher, J. S., III. 2000, in preparation
Dietz, R. D., Smith, J., Hackwell, J. A., Gehrz, R. D., & Grasdalen, G. L. 1986, AJ, 91, 758
Freedman, W., et al. 1994, ApJ, 427, 628
Gallagher, J. S., III & Smith, L. J. 1999, MNRAS, 304, 540
Gordon, S. M., Kirshner, R. P., Long, K. S., Blair, W. P., Duric, N., & Smith, R. C. 1998, ApJS, 117, 89
Green, D. A. 1984, MNRAS, 209, 449
Hansen, C. J., & Kawaler, S. D. 1994, Stellar Interiors: Physical Principles, Structure, and Evolution (New York: Springer)
Holtzman, J. A., Burrows, C. J., Casertano, S., Hester, J. J., Trauger, J. T., Watson, A. M., & Worthey, G. 1995, PASP, 107, 1065
Huang, Z. P., Thuan, T. X., Chevalier, R. A., Condon, J. J., & Yin, Q. F. 1994, ApJ, 424, 114
Iben, I., Jr. & Laughlin, G. 1989, ApJ, 341, 312
Kennicutt, R. C. 1984, ApJ, 277, 361
Kennicutt, R. C., Edgar, B. K., & Hodge, P. W. 1989, ApJ, 337, 761
Kronberg, P. P., Biermann, P., & Schwab, F. R. 1985, ApJ, 291, 693
Long, K. S., Blair, W. P., Kirshner, R. P., & Winkler, P. F. 1990, ApJS, 72, 61
Lynds, C. R., & Sandage, A. R. 1963, ApJ, 137, 1005
Marcum, P., & O'Connell, R. W. 1996, in ASP Conf. Ser. 98, From Stars to Galaxies: The Impact of Stellar Physics on Galaxy Evolution, ed. C. Leitherer, U. Fritze–von Alvensleben, & J. Huchra (San Francisco: ASP), 419
Matonick, D. M., & Fesen, R. A. 1997, ApJS, 112, 49
Matonick, D. M., Fesen, R. A., Blair, W. P., & Long, K. S. 1997, ApJS, 113, 333
Matthews, B. C., Wallace, B. J., & Taylor, A. R. 1998, ApJ, 493, 312
McCarthy, P. J., Heckman, T., & van Breugel, W. 1987, AJ, 92, 264
Meurer, G. R., Heckman, T. M., Leitherer, C., Kinney, A., Robert, C., & Garnett, D. R. 1995, AJ, 110, 2665
Milne, D. K., Caswell, J. L., & Haynes, R. F. 1980, MNRAS, 191, 469
Muxlow, T. W. B., Pedlar, A., Wilkinson, P. N., Axon, D. J., Sanders, E. M., & de Bruyn, A. G. 1994, MNRAS, 266, 455
O'Connell, R. W., Gallagher, J. S., III, Hunter, D. A., & Colley, W. N. 1995, ApJ, 446, L1
O'Connell, R. W., & Mangano, J. J. 1978, ApJ, 221, 62 (OM78)
Raymond, J. C. 1979, ApJS, 39, 1
Rieke, G. H., Lebofsky, M. J., Thompson, R. I., Low, F. J., & Tokunaga, A. T. 1980, ApJ, 238, 24
Rieke, G. H., Loken, K., Rieke, M. J., & Tamblyn, P. 1993, ApJ, 412, 99
Satyapal, S., Watson, D. M., Pipher, J. L., Forrest, W. J., Greenhouse, M. A., Smith, H. A., Fischer, J., & Woodward, C. E. 1997, ApJ, 483, 148
Shopbell, P. L., & Bland-Hawthorn, J. 1998, ApJ, 493, 129
Shull, J. M., Fesen, R. A., & Saken, J. M. 1989, ApJ, 346, 860
Stetson, P. B. 1987, PASP, 99, 91
Telesco, C. M. 1988, ARA&A, 26, 343
Woltjer, L. 1972, ARA&A, 10, 129
Yang, H., Skillman, E. D., & Sramek, R. A. 1994, AJ, 107, 651
Youngblood, A. J., & Hunter, D. A. 1999, ApJ, 519, 55